International Journal of Engineering Research & Technology (IJERT)
ISSN: 2278-0181
Vol. 10 Issue 08, August-2021

Finite Element Analysis of Fracture Properties of Reinforced Geopolymer Concrete Beams

Mariam Ghazy[1]
Professor
Structural Engineering Department
Tanta University, Tanta, Egypt

Metwally Abd Elaty[2]
Professor
Structural Engineering Department
Tanta University, Tanta, Egypt

Salah F. Taher[3]
Professor
Structural Engineering Department
Tanta University, Tanta, Egypt

Mohamed Elmasry[4]
Ph.D. candidate, Teaching Assistant
(corresponding author)
High Institute of Engineering
Elshorouk Academy, Egypt

Sherif Elwan[5]
Assoc. Professor
High Institute of Engineering
Elshorouk Academy, Egypt

Abstract:- **Nonlinear finite element method based on advanced three direction models is an economical tool and powerful which can be effectively used to simulate the true behaviour of concrete elements even under complex conditions. A 3 D nonlinear finite element analysis has been used to conduct an analytical study of the heat-cured alkali-activated fly ash-based geopolymer concrete specimens cast with polypropylene fibers. In the experimental part, ten notched beams were investigated in a three-point bending test. three notch height 0, 50, and 75 mm have been investigated at reinforcement ratios of 0, 0.07%, 0.17%, and 0.3%.**

This study aims to present a model suitable for analysing reinforced concrete notched beams using finite element methods. ABAQUS computer program version 6.16 is utilized in the analysis. The concrete was idealized by using the homogeneous solid elements, while the notch was modelled by using a planer shell and flexural steel reinforcement was modelled as a wire element by assuming a perfect bond between the concrete matrix and the flexural steel reinforcement rebar. The crack pattern is given by the finite element model similar to the experimental ones and the same trend of the load-displacement relation

Keywords-Geopolymer Concrete; Fracture mechanics; LEFM; XFEM; Smeared Crack, Discrete Crack, CDP

1. INTRODUCTION

Failures of elements and parts lead sometimes to cracks which can have catastrophic results, even if the stress level in a structure considered, perfect" can indicate a satisfactory design. The study of crack initiation and propagation is a complex subject. Identicating the main case concerning the propagation of cracks is considered in the Fracture Mechanics engineering field. Due to reduce cost and time otherwise expensive experimental tests, we can develop a powerful and reliable analytical techniques, such as finite element method (FEM). The finite element method may better simulate the experimental conditions such as the loading and deformation, support conditions of the actual experimental test. For example, engineers desire to

understand the conditions in which a pre-existing crack continues to propagate. Next, using Finite Element Analysis (FEA) to determine the stress at the tip of a pre-crack and investigated other fracture mechanics related characteristics. Thus, it uses the FM module for the ABAQUS finite element analysis software.

Finite element analysis (FEA) is an important tool in the study of fracture mechanics in elements and particular, Linear elastic fracture mechanics (LEFM) has been well-studied using methods such as Damage for Traction Separation Laws (TSL) and Concrete Damaged Plasticity Model (CDP) [10].

The investigation of crack propagation using Abaqus software uses a function, meaning that, firstly the stress state is being analyzed, then the crack propagation is deduced based on the results from the table Results environment.

Fiber geopolymer concrete (FGPC) is a type of eco-friendly concrete that may reduce the emission of a lot of carbon dioxide (CO_2) in the atmosphere and thus represents an alternative to cement concrete (CC) matrix. Its proven durability, mechanical and thermal properties are attractive features of GPC. Fiber reinforced composites is used to improve flexural strength and fracture toughness. fiber reinforced composite materials have been playing an important role in the rehabilitation and repair of damaged concrete and masonry structures, due to their high strength to weight ratio, corrosion resistance, and ease of application. It has been announced that adding reinforcing fibers to a brittle matrix helps to control and improve macro and micro-cracks diffusion through the material matrix by creating a bridging effect.

International Journal of Engineering Research & Technology (IJERT)
ISSN: 2278-0181
Vol. 10 Issue 08, August-2021

There are limited studies available in the literature on finite element modeling of GPC [2,5,7,9,11,12,13, 17,18,19,21,23, 25 and 26]. S. Nayak et al [19] study the fracture response of notched beams under 3-point bending is simulated using extended finite element method (XFEM) to determination of fracture characteristics. The notched beams of size 330 x 25x 75 mm were used. Y. Yin [24] using abaqus simulation to determine the concrete fracture parameters using three-point bending beams with specimen dimension and initial crack length 150 x 100 x 750 x 60 mm. The objective of this research is to investigate the performance of nonlinear models for analyzing the response of reinforced concrete notched beams, and compare the results with experimental crack beam approaches. In particular, the influence of the mesh size on load, deflection, concrete strain and mid span steel strain and local crack patterns will be investigated for these two finite element approaches.

2. EXPERIMENTAL DETAILS (Case Study)

The mix design for the geopolymer samples is listed in [17]. Cubes specimens were cast with dimensions 100x100x100 mm^3 for the compressive strength and concrete density. As well as, cylinder specimens with dimensions 100 x 200 mm^2 for the splitting tensile strength and the modulus of elasticity, respectively. Beam specimens were cast with dimensions 100x150x1000 mm^3 for the flexural strength. The casting and curing processes are explained in detail in the researcher's PHD thesis and [17 and 18]. Fig. 1 show the Typical notched beam specimen dimension. [17 and 18]

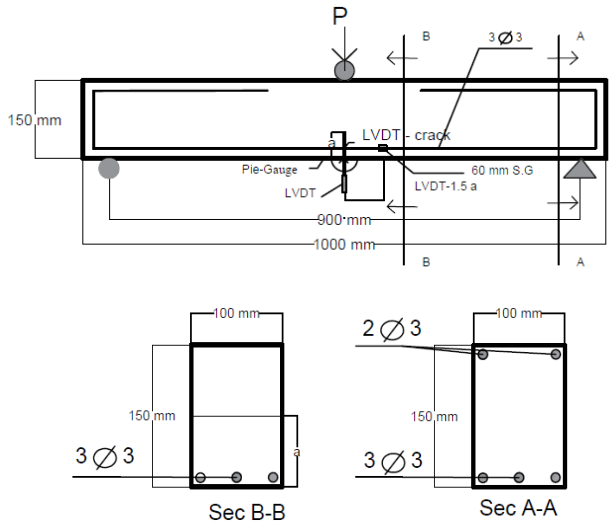

Fig. 1: Typical notched beam specimen dimension

The test specimens by [4,17 and 18] were continuous system is a notched beam with span equal to 100mm in both directions. Specimens' dimensions are series of 10 notched 100× 150× 1000mm beams with clear span between supporting beams equal to 900 mm in both directions. Notches were formed at the lower surface of the middle of 3 mm width and 50 and 75 mm heights. Details of specimens are illustrated in Fig. 1. All the beams are designated by two codes representing: Notch height–reinforcement bar diameter. With respect to reinforcement, plain FGPC, and reinforcing smooth 280/450 N/mm^2. steel bars diameters are 2, 3 and 4mm have been considered.

Three-Point Bending Single-Edge Notched Fracture test based on ASTM D5045-14 [4] was used to quantify the fracture parameters. Fig. 2 show the Test Specimen beam under loading. The mechanical properties of GPC samples determined after 28 days are listed in Table (1).

Table 1: Average properties of FGPC samples [17]

Slump (mm)	Concrete density (kg/cm^3)	Compressive Strength (MPa)*	Tensile strength (MPa)	Modulus of Elasticity (GPa)
100	2362	47.54	2.80	25.0

Fig.2: Test Specimen beam under loading

3. FINITE ELEMENT MODEL

ABAQUS (V 6.16) computer program is applied for analyzing all tested beams by [17 and 18]. Structural components corresponding to finite element representation, and elements designation in ABAQUS program will be represented below.

a) Modeling of the Material

Concrete

ABAQUS contains three models for modeling the nonlinear behavior of concrete. The available models are the concrete damage plasticity, the concrete smeared cracking and the brittle cracking model. In the current study, the concrete damage plasticity model (CDP) and Damage for Traction Separation Laws (TSL) have been used to model the concrete behavior, because it:

- Provides a general ability for modeling concrete matrix in all kinds of structures.
- Uses notion of isotropic elasticity in combination with compressive plasticity and isotropic tensile to appear the behavior of concrete.
- Can be model concrete reinforcement elements with defined reinforcing rebar.
- Comparison between the fracture methods and its crack extension

The Concrete Damage Plasticity model (CDP)

The model indicates that the main failure mechanisms are tensile cracking and compressive crushing of the concrete material indicated for 47.5 MPa Concrete in [23]. The model assumes that the concrete response is termed by damaged plasticity, as shown in Fig.3. [15 and 24]

In Figure 3, *fcr* indicates the value of uniaxial compressive strength of concrete, *ftr* indicates the value of uniaxial tensile strength of concrete, e_{cr} indicates the peak compressive strain corresponding to *fcr*, and *etr* indicates the peak tensile strain corresponding to *ftr*.

International Journal of Engineering Research & Technology (IJERT)
ISSN: 2278-0181
Vol. 10 Issue 08, August-2021

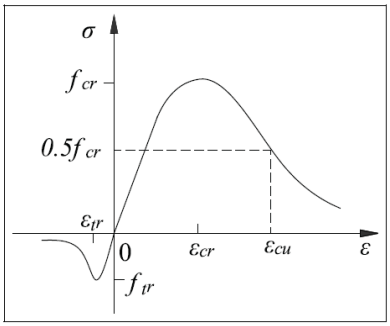

Fig. 3: The concrete response of uniaxial loading [24]

Damage for Traction Separation Laws model (TSL)

Abaqus allows for the modeling of adhesive layer using the traction-separation law in order to allow for the deboning failure mode. Abaqus provides two techniques for this purpose, the first is by using a cohesive element, and the second depends on using a surface based cohesive behavior.
The fracture energy is equal to the area under the load-deflection curve. One can identify the fracture properties as the cohesive interaction and choose either a linear or an exponential softening behavior. [22]

Flexural Steel Reinforcement

For the discrete model, three dimensional element used to model the flexural steel reinforcement. Two nodes are required for this element. Each node has three degrees of freedom, translations in the x, y, and z directions. The element is also capable of plastic deformation.

4. MATERIAL PROPERTIES

Concrete Elements

There are multiple parts of the material model for the concrete element as can be found, it used for all the concrete elements, and it is mean as linear isotropic for the elastic zone of the concrete, and multilinear isotropic for the plastic zone of the concrete. The elastic parameters required to establish the tension stress-strain curves are concrete elastic modulus, Ec, concrete tensile strength, f_{ct}, according to the experimental results E_c and f_{ct} were:

$$E_c = 30356.8\ MPa \quad \text{and} \quad fct = 2.8\ MPa$$

The Poisson's ratio of concrete is 0.2.

Concrete Damaged Plasticity Model Parameters

The CDP requires concrete tensile and compressive constitutive relationship, crushing and cracking damage parameters and special parameters such as dilation angle, eccentricity, biaxial loading ratio, the coefficient K and viscosity parameter. These parameters can be assigned to their commonly used values in Table (2). Dilation angle is related to the ratio of plastic volume change to plastic shear strain. The eccentricity is a small positive number that defines the rate at which the hyperbolic flow potential approaches its asymptote. f_{to}/f_{co} the ratio of initial equibiaxial compressive yield stress to initial uniaxial compressive yield stress. Viscosity parameter used for the visco-plastic regularization of the concrete constitutive equations. This parameter is ignored in Abaqus.
k, is proportional to the ratio of cohesion to the maximum cohesion of the material. The rationale of this assumption is that the plastic strain with stiffness degradation must be smaller than that without degradation, and the effect increases as degradation increases. the ratio of the plastic strain with stiffness degradation (ε^{-p}) to that without stiffness degradation (ε^{p}) [2 and 15]

$$\frac{f_{to}}{f_{co}} = 1.5 * (f_c^{-})^{-0.075} \qquad (1)$$

$$K = \frac{\varepsilon^{-p}}{\varepsilon^{p}} = \frac{\sigma}{f} \qquad (2)$$

in which f is either the tensile or compressive strength of concrete as appropriate.

Table (2) Concrete Damaged Plasticity Model Parameters

Dilation Angle	Eccentricity	f_{to}/f_{co}	K	viscosity parameter
31	0.1	1.16	0.667	0

Damage for traction separation law Model Parameters

The TSL requires concrete tensile and compressive constitutive relationship and the maximum principal stresses. The fracture parameters can be assigned to their commonly used Eqs. (3).
The maximum principal stress in this model is based on the uniaxial unconfined compressive strength (*fc*) and is denoted as τ_{max}. [16]

$$\tau_{max} = 0.6\sqrt{f_c}\ . \qquad (3)$$

Flexural Steel Reinforcement

The steel in the finite element models was identified to be an elastic-perfectly plastic material and identical in tension and compression.
It used for the longitudinal steel reinforcement in the beam and it is defined as linear isotropic for the elastic zone of the steel and bilinear isotropic to define the second part of the curve as a straight line. Bilinear isotropic material is also based on the von Mises failure criteria. The bilinear model requires the yield stress (fy). Also the modulus of elasticity (E), and the Poisson's ratio. Parameters needed to define the material models were:

$$E_c = 200000\ MPa \quad \text{and} \quad fy = 35\ MPa$$

The Poisson's ratio of steel is 0.3. the bond between reinforcement steel and concrete was assumed as a perfect bond.

Element, Meshing and Boundary Conditions

An eight-node linear brick, reduced integration, hourglass control element was used to model the concrete as shown in Fig. 4. A two-node linear 3D line element was used to model the steel bars and stirrups. This element transmits only axial load. Numerical trials have been selected the ideal mesh size using different mesh sizes (1–3 cm) to. Fine mesh consisting of elements with maximum area of 1.0 cm^2 is used because a finer mesh does not show significant differences in results. The two supports were modeled as hinged and roller supports. The relation between the concrete and the steel reinforcement was assumed to have full bond and was modeled by the embedded region constraint.

International Journal of Engineering Research & Technology (IJERT)
ISSN: 2278-0181
Vol. 10 Issue 08, August-2021

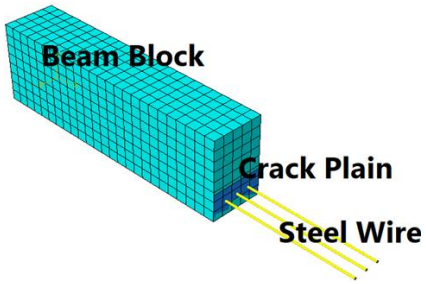

Fig. 4: 3D modelling of a reinforced concrete notched beam

5. VALIDATION OF ANALYTICAL FINITE ELEMENT RESULTS

Comparison between Numerical Analysis and Experimental Results

Table (3) summered and illustrates the maximum flexure force, corresponding vertical deflection for experimental results and maximum concrete and mid-span steel strain experimental and finite element results which was extracted from the abaqus finite element analysis. Figs. 5 and 6 show examples of cracking experimental beam at yielding stage and cracking propagation at Analytical beam, respectively. Figs. 7,8,9,10,11, and 12 show the typical view, the deformed shape, examples of concrete stress, deformed shape of cracked FEM Beam and Crack Stress, respectively.

Fig.5: Example of Cracking propagation of experimental beam

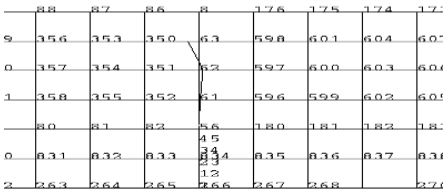

(a) CDP

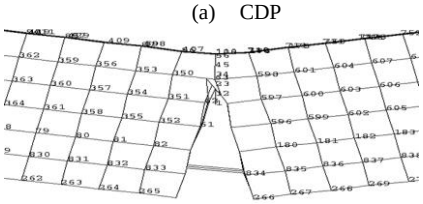

(b) TSL

Fig.6: Example of Cracking propagation at FE beam

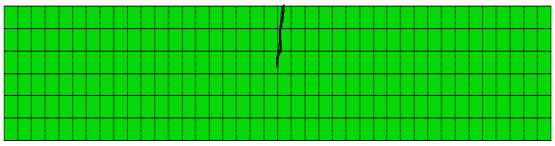

(a) Beam without rebar

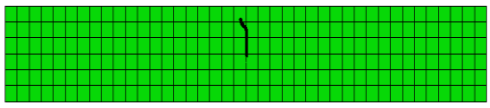

(b) Beam with rebar

Fig.7 : Typical View of cracked FEM Beam

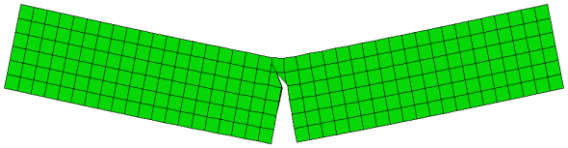

(a) Beam without rebar

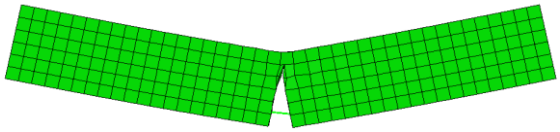

(b) Beam with rebar

Fig.8: Typical Deformed shape of cracked FEM Beam

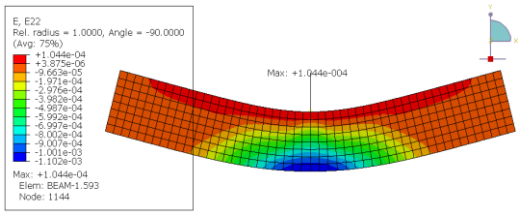

(a) CDP

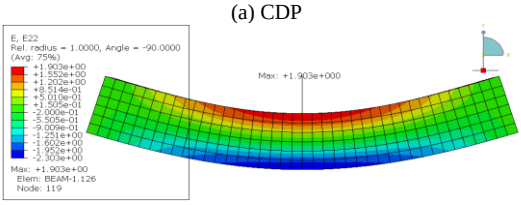

(b) TSL

Fig. 9: Example of concrete strain of cracked FE Beams (0-3)

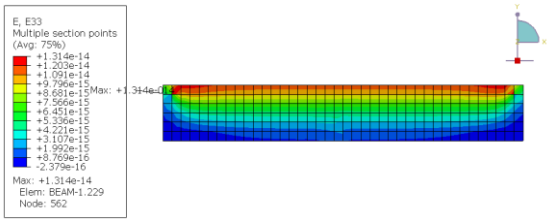

(a) CDP

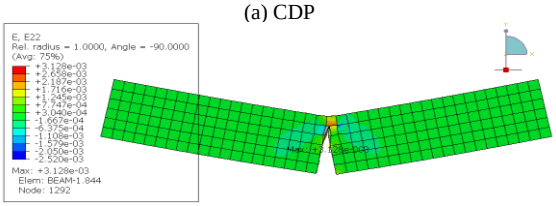

(b) TSL

Fig. 10: Example of concrete stress of cracked FE Beams (75-3)

International Journal of Engineering Research & Technology (IJERT)
ISSN: 2278-0181
Vol. 10 Issue 08, August-2021

Table 3 : Summary For Experimental and Finite Element Results

Beam ID	Experimental [17]				CDP				TSL			
	P (KN)	Max. Defl. (mm)	Max Concrete Strain (Micro strain)	Mid Span Steel Strain (Micro strain)	P (KN)	Max. Defl. (mm)	Max Concrete Strain (Micro strain)	Mid Span Steel Strain (Micro strain)	P (KN)	Max. Defl. (mm)	Max Concrete Strain (Micro strain)	Mid Span Steel Strain (Micro strain)
0-0	8.2	8.6	8387	0	8.5	11.9	8409	0	5.6	11.6	2848	0
0-3	8.9	10	5561	3829	8.4	10.6	5438	3801	3.2	6.3	3225	3673
50-0	2.4	5	5362	0	2.6	4.3	4840	0	1.7	3.1	3159	0
50-2	3.1	14.9	3269	1755	2.5	7.7	3758	818	3.6	5.5	2824	1716
50-3	8.5	8.5	1212	3976	10.5	7.7	1148	2377	9.4	7.5	3124	3174
50-4	15.3	7.8	3118	3311	18.0	6.3	3160	732	13.9	4.5	2574	3206
75-0	2.2	5.0	4354	0	2.6	4.93	4852	0	1.6	3.1	2830	0
75-2	3.2	8.8	1052	1755	1.9	8.5	557	983	3.2	4.3	938	1716
75-3	7.8	12.5	3077	3676	4.8	13.3	2521	2178	7.0	15.1	2498	3174
75-4	12.9	14.3	1549	3317	9.5	10.5	1264	722	8.3	9.8	1633	3409

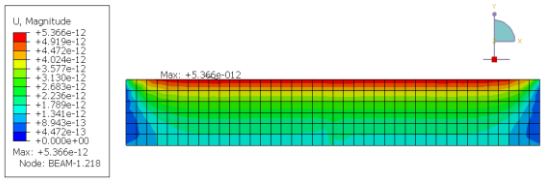

(a) CDP

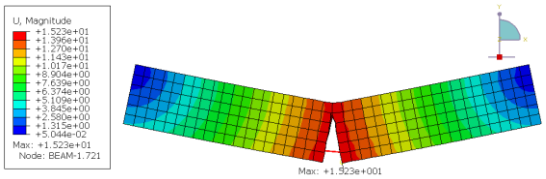

(b) TSL

Fig. 11: Example of Deformed shape of cracked FE Beams (50-3)

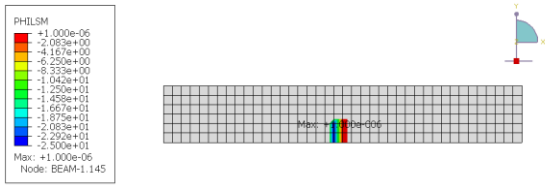

(a) CDP

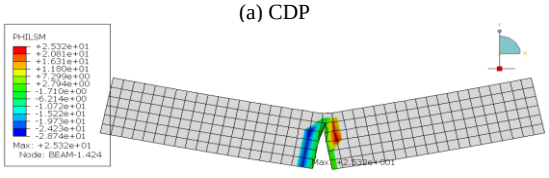

(b) TSL

Fig.12: Example of Crack Stress of cracked FEM Beam (75-3)

Figure 13 show the relation between load-mid span deflections in experimental and finite element model using ABAQUS. The differences between the finite element and the experimental results in the concrete deformations were considered due to both the crushing technique in ABAQUS and the limitations of concrete to deform with cracks. In general, both experimental and finite element models and responses have the same trend. It can be investigated that for the FGPC specimens (without reinforcement), increasing the notch height decreased the load-carrying capacity by 64%. The presence of reinforcement improved, as expected, the flexural capacity compared with the FGPC beams without reinforcement by 30% and 35% for 3 and 4mm rebar's diameter respectively.

Figure 14 shows the results in the finite element and experimental model. The differences between experimental and FE in terms of concrete deformations were considered due to both the limitations of concrete to deform with cracks and the crushing technique in ABAQUS. In general, the experimental and FE responses have the same trend. Fig. 14-a shows the failure load for 50 and 75mm notch height with various reinforcement ratios. The bar chart reflects that the Finite Element methods give results closer to the laboratory results by a deviation of 15% in the case of failure loads for all reinforced rebar.

According to using two methods in FE analysis, Figure 15 gives the relationship between the two methods, based on the same characteristics of the model spacemen, it can note that the higher the reinforcement ratio in the samples the less the difference between them. It can note that the average difference between the finite element methods results is to reduce as the reinforcement ratio increased from 0% to 0.3%. Figure 15 shows the Load–energy curves for 50 and 75mm notch height with various reinforcement ratios.

International Journal of Engineering Research & Technology (IJERT)
ISSN: 2278-0181
Vol. 10 Issue 08, August-2021

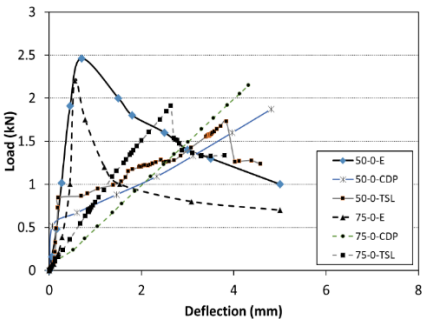

(a) GPC without Reinforcement

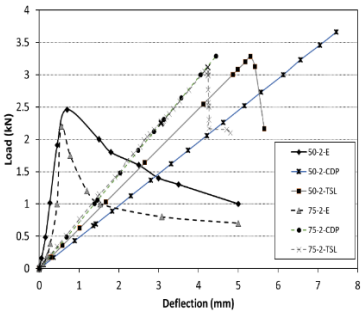

(b) 0.07% Reinforcement Ratio

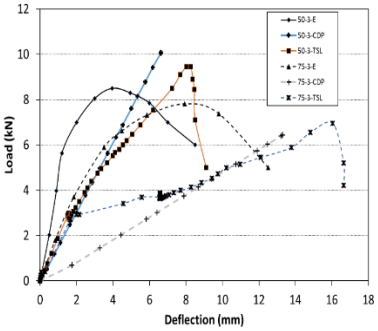

(c) 0.17% Reinforcement Ratio

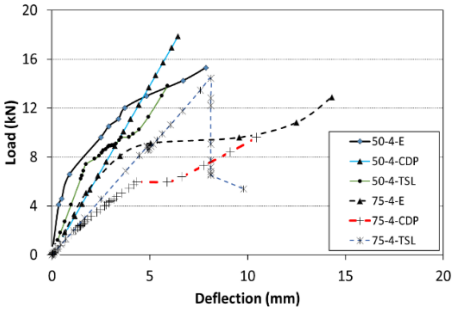

(d) 0.3% Reinforcement Ratio

Fig. 13: Comparison between Load- Deflection curve in FEM and experimental method

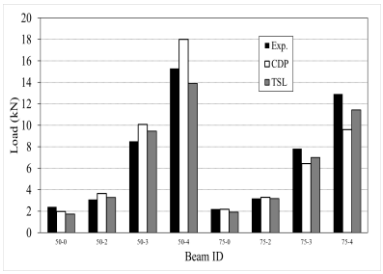

(a) Failure load

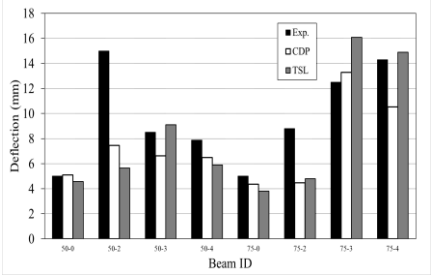

(b) Max mid span deflection

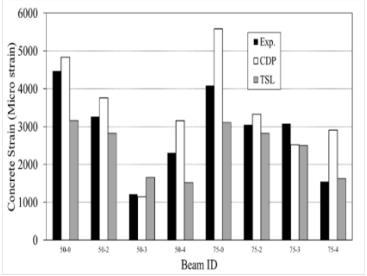

(c) Max. Concrete Strain

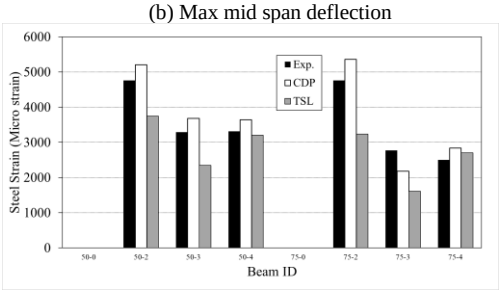

(d) Mid-Span Steel Strain

Fig. 14: Comparison between FEM and experimental method

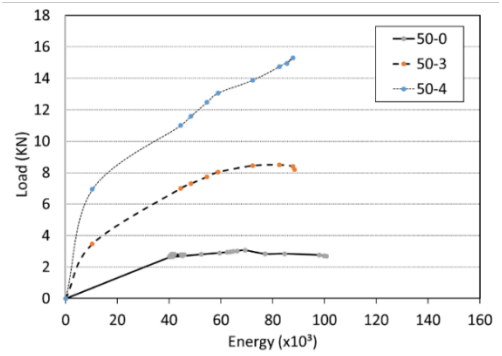

(a) 50 mm notch

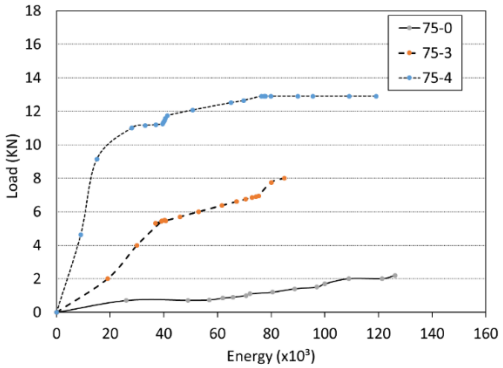

(b) 75 mm notch

Fig. 15: Comparison between fracture energy with different reinforced ratio according to FEM

International Journal of Engineering Research & Technology (IJERT)
ISSN: 2278-0181
Vol. 10 Issue 08, August-2021

J-K relationship curve

Figure 16 shows the stress intensity factors distributions according to J-integral values. The notch height had significant proportional effect on K- factor where specimens with 75 mm notch height experienced less values than those with 50mm at the same load level.

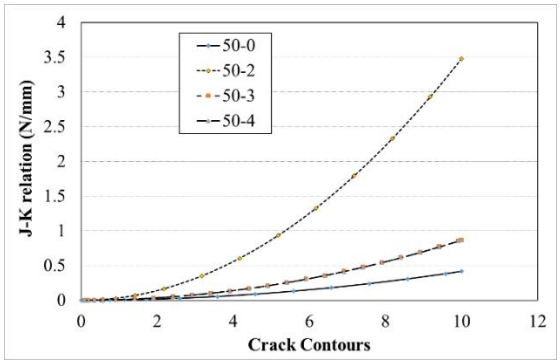

(a) 50 mm notch

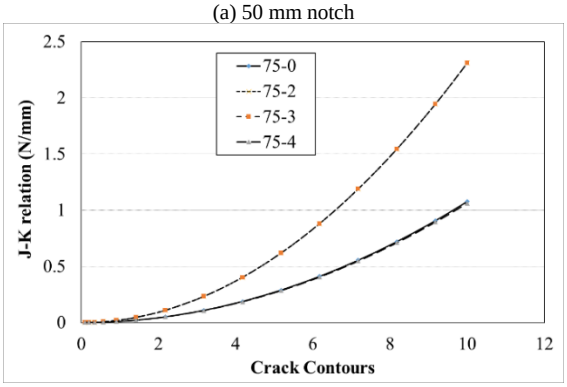

(b) 75 mm notch

Fig. 16: J-K curve of specimen with various notch height

Stress intensity factor (K) based on crack path

Figure 18 shows the stress intensity factors (Eq.4) distributions according to true distance along the crack path. The stresses in beams without reinforcement indicated normal distribution along the path of the crack. The final values differed in accordance with the load carrying capacity of each beam.

$$S_{Ii} = \frac{K_{ic}}{\sqrt{2\pi a}} \qquad (4)$$

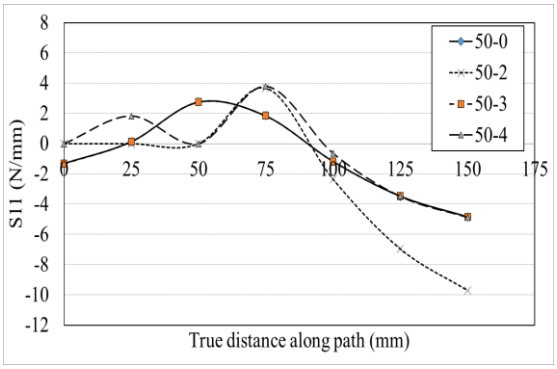

(a) 50 mm notch

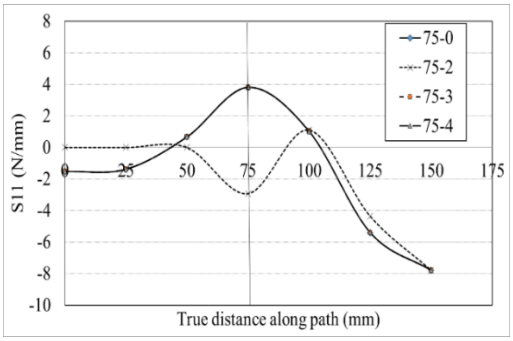

(b) 75 mm notch

Fig.18: Crack Path Stresses of specimen with various notch height

6. LINEAR ELASTIC FRACTURE MECANICS ANALYSIS (LEFM)

Based on displacement control loading of specimens, fracture toughness (K_{IC}), fracture energy (G_F), characteristic length (l_{ch}), brittleness (B) and J- Integral (J_{IC}) were estimated.

Development of the constitutive model for a material requires its fracture parameters which were used to be quantified analytically for cement concrete (Eq. 5) [17,18 and 27] as following:

$$K_{IC} = \frac{3Pl}{2bd^2} * \sqrt{a} * (1.93 - 3.07\,A + 14.53\,A^2 - 25.11\,A^3 + 25.8\,A^4) \qquad (5)$$

Where: $A = (a/d)$, a is the depth of the notch (mm), d is the depth of the beam (mm), b is the width of the beam (mm), P is the maximum load (N) and l is the span length of the beam (mm).

The G_F were estimated by three different models (Eqs. 6, 7 and 8) by [17,18 and 25], respectively as following:

$$G_F = \frac{w_o + mg\delta_0}{A_{lig}} \qquad (6)$$

$$G_F = \int_{\delta=0}^{\delta=\delta_{lim}} \sigma \, d\delta \qquad (7)$$

Where: $\sigma = \frac{3Pl}{2b(h-a_0)^2}$, a_0 is the depth of the notch (mm), d is the depth of the beam (mm), b is the width of the beam (mm), P is the maximum load (N) and l is the span length of the beam (mm).

$$G_F = \frac{{K_{IC}}^2}{E} \qquad (8)$$

The l_{ch}, B and J_{IC} were estimated by using the formulas (Eqs. 9, 10 and 11) by [19 and 26], respectively as following:

$$l_{ch} = \frac{G_F\,E}{{f_t}^2} \qquad (9)$$

$$B = \frac{L\,{f_t}^2}{G_F\,E} \qquad (10)$$

Where: G_F is the fracture energy, E is the modulus of elasticity, ft is the tensile strength and L is the size of the test specimen.

$$J_{IC} = \frac{K_{IC}}{E} \qquad (11)$$

7. PREDICTION OF FRACTURE PARAMETERS ACCORDING TO FINITE ELEMENT RESULTS BY (LEFM)

Table 4 lists the computed parameters according to the aforementioned expressions for the specimens 50-0 and 75-0 specifically.

International Journal of Engineering Research & Technology (IJERT)
ISSN: 2278-0181
Vol. 10 Issue 08, August-2021

Table 4: Fracture parameters of analysis methods without reinforcement

Parameter		K_{IC} N/mm$^{3/2}$	G_F N/mm			l_{ch} m	B	J_{IC} N/mm
Notch Height	Method							
	Eq.	(5)	(6)	(7)	(8)	(9)	(10)	(11)
50	Exp.	44.84	5.18	16.61	0.10	21.36	0.07	3.17
	CDP	48.31	3.60	15.42	0.09	10.41	0.09	1.93
	TSL	31.54	2.19	7.33	0.04	6.33	0.14	1.26
75	Exp.	114.37	4.36	21.65	0.63	10.40	0.09	5.55
	CDP	103.46	3.34	22.30	0.43	9.66	0.09	4.14
	TSL	83.18	1.22	11.90	0.28	3.53	0.26	3.32

It is obvious that the fracture toughness is notch height dependent. In addition, other G_F dependent parameters given by equations are notch size dependent. In addition, there is a great discrepancy between the predictions of the fracture energy after each formula. It can note that the "by definition" formula (Eq. 6) is the most valid as the nonlinearity is associated with the behavior of FGPC. [8]

From table 4 the CDP method, the fracture parameters: fracture toughness (K_{IC}) and fracture energy (G_F), characteristic length (l_{ch}), brittleness (B) and J- integral (J_{IC}) achieve 107%,70%,49%,129% and 61% of experimental method behavior for 50 mm and increased to 77%,93% and 75% with increased the notch height 75 mm for G_F, l_{ch} and J_{IC} and decreased to 90% for K_{IC}.
For the TSL method, the fracture parameters: fracture toughness (K_{IC}) and fracture energy (G_F), characteristic length (l_{ch}), brittleness (B) and J- integral (J_{IC}) achieve 71%,43%,32%,200% and 40% of experimental method behavior for 50 mm and increased to 288% and 60% with increased the notch height 75 mm for B and J_{IC} and decreased to 28% for G_F.

8. VERIFICATION OF FRACTURE PARAMETERS BETWEEN FEM and LEFM

Table (5) shows the computed parameters according to the experimental, LEFM expressions and ABAQUS finite element modeling for various notched beam specimens without reinforcement.

Table (5): Comparison of Fracture parameters of the notched beam according difference methods

Parameter		Equation	K_{IC} N/mm $^{3/2}$	J_{IC} N/mm
Notch Height	Method			
50 mm	Experimental	(5)	44.84	3.17
	FEM(LEFM)	(5)	31.54 – 48.31	1.26 – 1.93
	FEM (Abaqus)	(4)	48.9	1.64
75mm	Experimental	(5)	114.37	5.55
	FEM(LEFM)	(5)	83.18 – 103.46	3.32 – 4.14
	FEM (Abaqus)	(4)	82.5	4.45

9. EFFECT OF VARIOUS REINFORCEMENT RATIO ON FRACTURE BEHAVIOUR ACCORDING FEM

According to the analytical formulation of the bridged crack model, the overall behavior is a function of the reinforcement "brittleness number" N_P, defined on the geometrical and mechanical parameters. a "Brittleness Number", N_P represents a ductility parameter (Eq.12) Therefore, a brittle response with a softening branch after the peak cracking load, is expected for low values of N_P by increasing its value. it ranges from 0.1 to 15 as ductile response is predicted, with a hardening behavior after the cracking load and a large inelastic displacement due to steel yielding.
In particular, the cracking load is a decreasing function of the dimensionless number s, (Eq.13). Therefore, for a fixed value of N_P, by increasing the value of S ranges from 0.2 to 3.0. the response becomes more and more stable. In general, a transition from brittle to ductile response is obtained by increasing N_P and/or S. [1]

$$N_p = \frac{A_s}{b\,h}\,\frac{f_{yk}\,h^{0.5}}{K_{IC}} \tag{12}$$

$$S = \frac{K_{IC}}{f_{ctm}\,h^{0.5}} \tag{13}$$

where: fyk steel yield strength, b width of beam, h overall depth of beam, K_{IC} concrete fracture toughness, A_s area of tension reinforcement.

The ratio M_P/M_F, would be indicative of the effect of reinforcement on fracture behavior given in Eq. (14). [1]

$$\frac{M_P}{M_F} = \frac{r^*\left(\frac{c}{h},\xi\right)\; Y_M(\xi)}{{N_P}^{-1} + Y_P\left(\frac{c}{h},\xi\right)\frac{P}{P_P}} \tag{14}$$

Where : $Y_P\left(\frac{c}{h},\xi\right) = \frac{2}{\sqrt{\pi\xi}}\left\{\frac{3.52\,(1-\frac{c}{a})}{(1-\frac{a}{h})^{3/2}} - \frac{4.35-5.28\frac{c}{a}}{\left(1-\frac{a}{h}\right)^{\frac{3}{2}}} + \left[\frac{1.3-0.3\,(\frac{c}{a})^{3/2}}{(1-\left(\frac{c}{a}\right)^2)^{0.5}} + 0.83 - 1.76\,c/a\right]\left[1-\left(1-\frac{c}{a}\right)a/h\right]\right\}$,

$r^*\left(\frac{c}{h},\xi\right) = \frac{\int_{c/h}^{\xi} Y_M(\xi)\,Y_P\left(\frac{c}{h},\xi\right)d\xi}{\int_0^{\xi} {Y_M}^2(\xi)\,d\xi}$ and $Y_M(\xi) = K_{IM}\,\frac{b\,h^{1.5}}{M}$

as M_F is critical moment of un-reinforcement beam, M_P plastic moment according to the elastic-perfectly plastic

International Journal of Engineering Research & Technology (IJERT)
ISSN: 2278-0181
Vol. 10 Issue 08, August-2021

reinforcement, *a* notch height, *h* overall depth of beam, c reinforcement cover, *b* width of beam, crack factor $\xi = a/h$, *M* plastic moment, K_{IM} concrete fracture toughness. Table 6 and Figs. 19 and 20 show the computed parameters according to the expressions mentioned in (Eqs.12 and 14) for the notched beam specimens with reinforcement at 0.07%, 0.17% and 0.3%.

From table 6, It can be noticed that CDP specimen achieved 102 % of experimental specimen for all notch height. Using TSL method achieved 70% and 80% of experimental specimen for 50 mm and 75 mm notch height.

Table 6: Comparison of Fracture parameters of the notched beam specimens

Parameter			K_{IC} N/mm$^{3/2}$	N_P	S	M_p/M_f
Notch Height	Method	Beam ID				
		Eq.	(5)	(12)	(13)	(14)
50	Exp.	50-2	44.84	0.67	1.25	0.54
		50-3		2.09	1.25	0.77
		50-4		4.10	1.25	0.85
	CDP	50-2	48.31	0.62	1.34	0.53
		50-3		1.94	1.34	0.75
		50-4		3.80	1.34	0.84
	TSL	50-2	31.54	0.95	0.88	0.62
		50-3		2.97	0.88	0.81
		50-4		5.82	0.88	0.87
75	Exp.	75-2	114.37	0.26	2.89	0.21
		75-3		0.90	2.89	0.55
		75-4		1.61	2.89	0.77
	CDP	75-2	103.46	0.29	2.87	0.23
		75-3		0.91	2.87	0.55
		75-4		1.78	2.87	0.82
	TSL	75-2	83.18	0.36	2.31	0.27
		75-3		1.13	2.31	0.63
		75-4		2.21	2.31	0.91

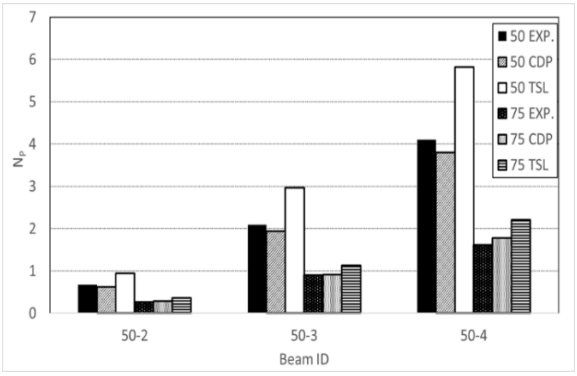

Fig.19: Comparison between Brittleness number (N_P)with difference methods

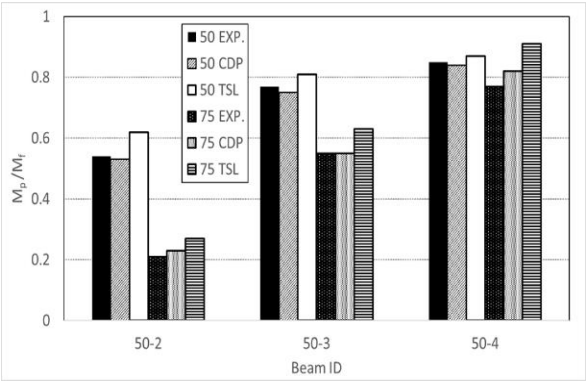

Fig.20: Comparison between (Mp/M_F) Ratio with difference methods

Figure 19 shows the results of the N_p for various reinforcement ratio of different beam specimens. It can be noticed that CDP specimen achieved 93% and 110% of experimental specimen for 50 mm and 75 mm notch height. Using TSL method achieved 140% of experimental specimen for all notch height. Figure 20 shows the results of the Mp/M_f ratio for various reinforcement ratio of different beam specimens. It can be noticed that CDP specimen achieved 105% of experimental specimen for all notch height. Using TSL method achieved 98 %. and 120% of experimental specimen for 50 mm and 75 mm notch height.

CONCLUSIONS

The Finite element model is performed based on the present test geometry and compared with the experimental results. Based on this investigation, the following conclusions can be drawn:

- ABAQUS computer program was used to develop a nonlinear analysis of three dimensional reinforced concrete beams under concentric increasing loads to simulate the behavior of experimental beams.
- Efficiency of the proposed finite element model for the reinforced concrete beams with notch, was proved from the comparison of the finite element model results with experimental results.
- Nonlinear finite element method based on advanced 3D models is a relatively economical tool and powerful. the finite element results can be effectively used to simulate the true behavior of reinforced concrete beams even under complex conditions.
- The crack pattern given by finite element model almost similar to the experimental ones and the same trend of the load-displacement response.
- Damage for Traction Separation Laws is the best method to represent the fracture mechanics model which achieve the experimental results.
- The average difference between the experimental and FEM results is 15% for all notch height and reinforcement ratio.
- The average difference between the finite element methods is reduce as reinforcement ratio increased from 0% to 0.3%.

International Journal of Engineering Research & Technology (IJERT)
ISSN: 2278-0181
Vol. 10 Issue 08, August-2021

- The Concrete Damage Plasticity method achieved the fracture parameters of experimental results for beam specimens.
- The finite element methods achieved the experimental results for Np and Mp/M_f ratio for reinforcement beam specimens.

ACKNOWLEDGEMENTS

This investigation is part of the Ph.D. research of the forth author at the Faculty of Engineering, Tanta University. The technical support and facilities provided by the Strength of Materials Laboratory, Structural Engineering Department; Tanta University to purse this research is appreciated.

REFERANCES

[1] A.Bosco, A. Carpinteri, Fracture mechanics evaluation of minimum reinforcement in concrete structure, In Applications of Fracture Mechanics to Reinforced Concrete, Elsevier Applied Science, London, 1992, pp. 347-377. https://doi.org/10.1201/9781482296624-14

[2] A.C. Ganesh, M. Muthukannan, Finite Element Analysis over Geopolymer Concrete using Abaqus, International Journal of Engineering and Advanced Technology (IJEAT), Volume-9, December 2019. https://doi.org/10.35940/ijeat.A1024.1291S419

[3] ABAQUS 6.11, User's Manual, Dassault Systèmes Simulia Corp., Providence, RI, USA.

[4] ASTM D 5045-14, Standard Test Methods for Plane-Strain Fracture Toughness and Strain Energy Release Rate of Plastic Materials, West Conshohocken, PA: ASTM International, 2014.

[5] D. Hardjito, Studies on Fly Ash-Based Geopolymer Concrete, PHD Thesis, Curtin University of Technology,2005.

[6] E.J. Barbero, Finite Element Analysis of Composite Materials Using Abaqus, Taylor & Francis Group, LLC, 2013.

[7] H.T. Nhabih, A.M. Hussein, M.M. Salman, Study a structural behavior of eccentrically loaded GFRP Reinforced Columns Made of Geopolymer Concrete, Civil Engineering Journal, Vol. 6, No. 3, March, 2020. https://doi.org/10.28991/cej-2020-03091492

[8] J.E. Srawley, W.F. Brown, Fracture toughness testing methods. In: Fracture toughness testing and its applications, ASTM STP 381, American Society for Testing and Materials, 1965, pp. 133–196. https://doi.org/10.1520/STP381-EB

[9] K. Uma., R. Amerada, R. Venkatasubramani, Experimental investigation and analytical modeling of reinforced geopolymer concrete beam, International Journal of Civil and Structural Engineering, Vol. 2, No 3, 2012, pp 817-827.

[10] M Hillerborg, M. Moder, P.E. Petersson, Analysis of crack formation and crack growth in concrete by means of fracture mechanics and finite elements, Cement and Concrete Research, (6), 1976, pp. 773-782. https://doi.org/10.1016/0008-8846(76)90007-7

[11] M. Jenifer, S. Kumar and C. Devadass, Fracture Behavior of Fiber Reinforced Geopolymer Concrete, International Journal of Advanced Technology in Engineering and Science www.ijates.com , Vol 3,2015. https://doi.org/10.18520/cs/v113/i01/116-122

[12] M.S. Midhun, T.D. Gunneswara Rao and T. Srikrishna, Mechanical and fracture properties of glass fiber reinforced geopolymer concrete, Advances in Concrete Construction, Vol. 6, No. 1, 2018, pp. 29-45. https://doi.org/10.12989/acc.2018.6.1.029

[13] P. Nath, P.K. Sarker, Fracture properties of GGBFS-blended fly ash geopolymer concrete cured in ambient temperature, Materials and Structures,2017. https://doi.org/10.1617/s11527-016-0893-6

[14] P. Sarker, R. Haque and K. Ramgolam, Fracture behavior of heat cured fly ash based geopolymer concrete, Material and Design 44, 2013, pp. 580-586. https://doi.org/10.1016/j.matdes.2012.08.005

[15] Q.Raza, A. Khan, A. Ahmad, Numerical Investigation of Load-Carrying Capacity of GFRP-Reinforced Rectangular Concrete Members Using CDP Model in ABAQUS, Advances in Civil Engineering , Hindawi, Vol. 2019, https://doi.org/10.1155/2019/1745341.

[16] R. Borst, J. Remmers and M.A. Abellan, Discrete vs smeared crack models for concrete fracture: bridging the gap, International Journal for Numerical and Analytical Methods in Geomechanics Int, 2004, pp.583–607. https://doi.org/10.1002/nag.374

[17] S. F. Taher, M.F. Ghazy, M.A. Abd Elaty, M. Elmasry and S. Elwan, Exploratory Scrutiny on Fracture of Lightly Reinforced Fiber Geopolymer Concrete Notched Beams, International Innovative Building Materials Conference, HBRC,2018.

[18] S. F. Taher, M.F. Ghazy, M.A. Abd Elaty, M. Elmasry and S. Elwan, Identification of Fracture Parameters of Fiber Reinforced Concrete Beams Made of Various Binders, Case Studies in Construction Materials 15(1),2021. https://doi.org/10.1016/j.cscm.2021.e00573

[19] S. Nayak, A. Kizilkanat, N. Neithalath, S. Das, Experimental and Numerical Investigation of the Fracture Behavior of Particle Reinforced Alkali Activated Slag Mortars, ASCE's Journal of Materials in Civil Engineering,2020. https://doi.org/10.1061/(ASCE)MT.1943-5533.0002673

[20] S.P. Shah, Application of Fracture Mechanics to Cementitious Composites, Advanced Research Workshop, Northwestern University, USA, September (4-7),1984.

[21] S.R. Deepa, R. Abraham, N. Ganesan and D. Sasi, Fracture Properties of Fibre Reinforced Geopolymer Concrete, International Conference on Innovations in Civil Engineering, (9-10 May),2013.

[22] Y. Dere, M. Koroglu, Nonlinear FE Modeling of Reinforced Concrete, International Journal of Structural and Civil Engineering Research Vol. 6, No. 1,2017. https://doi.org/10.18178/ijscer.6.1.71-74

[23] Y. Li, N. Xu, Tu J., G. Mei, Comparative modelling of crack propagation in elastic– plastic materials using the mesh free local radial basis point interpolation method and extended finite-element method, Royal Society Open Science,6,2019. https://doi.org/10.1098/rsos.190543

[24] Y. Xiao, Z Chen, et al, "Concrete plastic-damage factor for finite element analysis: concept, simulation, and experiment", Advances in Mechanical Engineering, Vol. 9, 2017, pp 1–10. https://doi.org/10.1177/1687814017719642

[25] Y. Yin, Y. Qiao, S. Hu, Determining concrete fracture parameters using three-point bending beams with various specimen spans", Theoretical and Applied Fracture Mechanics 107,2020. https://doi.org/10.1016/j.tafmec.2019.102465

[26] Z. Hua, Y. Xiao, H. Zhu, S. Hua and Y. Chen, Preparation and mechanical properties of polypropylene fiber reinforced calcined kaolin-fly ash-based geopolymer, Journal of Center South University Technology 16,2009, pp 49–52. https://doi.org/10.1007/s11771-009-0008-4

[27] Z.P. Bazant, J. Planas, Fracture and size effect in concrete and other quasi-brittle materials", CRC Press, 1997. https://doi.org/10.1201/9780203756799